Introduction

The appropriate DNA damage response that monitors and maintains genomic integrity is considered to be a critical barrier against tumorigenesis. Tumor suppressor p53 plays a pivotal role in the regulation of the DNA damage response. p53 is divided into three chracteristic functional domains, including the NH_2-terminal transactivation domain (TA), the central sequence-specific DNA-binding domain (DB) and the COOH-terminal oligomerization domain (OD). As expected from its structural property, p53 acts as a nuclear transcription factor and has the ability to transactivate numerous target genes implicated in the induction of cell cycle arrest ($p21^{WAF1}$ and *14-3-3σ*), DNA repair (*GADD45*), cellular senescence ($p21^{WAF1}$) and/or apoptotic cell death (*BAX*, *PUMA* and *NOXA*) [1–3]. Among these cellular processes, the promotion of apoptotic cell death has a prominent role in tumor suppression by eliminating cells with seriously damaged DNA. Upon cellular insult, such as DNA damage, oncogene activation and hypoxia, p53 is quickly activated by sequential post-translational modifications, including phosphorylation (Ser-15, Ser-20 and Ser-46) and acetylation (Ace-373 and Ace-382), thereby exerting its pro-apoptotic function via the subsequent transactivation of its target genes [1–3].

Unfortunately, p53 is mutated and loses its tumor-suppressive function in approximately half of human cancerous cells [4–6]. Over 90% of *p53* mutations are detectable within the genomic region encoding its central sequence-specific DNA-binding domain, suggesting that the sequence-specific transactivation activity of p53 is tightly linked to its pro-apoptotic function. By contrast to a short-lived wild-type p53, mutant p53 shows a prolonged half-life [3]. Additionally, mutant p53 aquires an oncogenic potential and also displays a dominant-negative behavior against wild-type p53 [7]. Moreover, cancerous cells expressing p53 mutant sometimes exhibit chemoresistant phenotypes [7,8]. Of note, mutant p53 transactivates myriad of genes involved in many different aspects of tumorigenesis such as *MYC*, *EGFR* and *MDR1* [8]. p73 is a member of p53 tumor suppressor family and acts as a negative regulator of tumorigenesis by inducing cell cycle arrest and/or apoptotic cell death via its ability to transactivate overlapping set of p53-target genes [9,10]. Similar to p53, p73 has been shown to accumulate in response to certain DNA damaging agents such as cisplatin and adriamycin (ADR) and to play a crucial role in the regulation of DNA damage response [11]. It has been reported that DNA damage-mediated transcriptional activation of *p73* is modulated by E2F-1 [12–14]. Importantly, *p73* produces two distinct gene products, including a transactivation domain-containing isoform (TAp73) and a transactivation-deficient NH_2-terminally truncated isoform (ΔNp73). ΔNp73 arises from the alternative promoter usage [15]. Although *p73* is rarely mutated in human cancerous cells [16], *TAp73*-deficient mice showed an increased susceptibility to spontaneous and carcinogen-induced tumors with a peculiar promotion of lung adenocarcinomas, implying that TAp73 possesses a tumor-suppressive capability [17]. It is worth noting that TAp73 is required for p53-dependent apoptotic cell death, whereas TAp73 alone has the ability to induce apotic cell death in the absence of wild-type p53 [18]. By contrast, ΔNp73 lacking the NH_2-terminal transactivation domain has an oncogenic function and acts as a dominant-negative inhibitor toward TAp73, as well as wild-type p53 [15,19]. Thus, the intracellular balance between the amounts of anti-apoptotic ΔNp73 and pro-apoptotic p53/TAp73 might be a critical determinant of cell fate. The mammalian runt-related transcription factor (RUNX) family is composed of three members, including RUNX1, RUNX2 and RUNX3. RUNX family members contain an evolutionarily conserved 128-amino acids runt domain, which is required for specific DNA-binding (ACC(A/G)CA) and heterodimerization with its cofactor CBFβ (core-binding factor β) [20,21]. CBFβ does not bind directly to DNA but enhances RUNX proteins binding to DNA [22]. Among the RUNX family members, RUNX2 was shown to play a key role in the regulation of proper osteoblast differentiation and bone formation [23,24]. By contrast to RUNX2, RUNX1 and RUNX3 are known to act as essential regulators of hematopoietic and gastric development, respectively [25–28]. Indeed, *RUNX2*-deficient mice completely failed to form mineralized bone [23,24] and mice overexpressing RUNX2 displayed osteopenia with multiple fractures [29]. Consistent with these observations, RUNX2 transactivates various target genes involved in the promotion of osteogenic differentiation, such as *type 1 collagen*, *osteopontin* and *osteocalcin* [30,31].

Alternatively, there is growing evidence to suggest that RUNX2 has a pro-oncogenic function in a wide variety of cells. For example, overexpression of RUNX2 in transgenic mice was found to predispose mice to lymphoma [32]. Intriguingly, Browne *et al.* [33] reported that RUNX2 induces the expression of pro-survival *Bcl-2* and thus contributes to the development of malignant phenotypes in prostate cancer cells. Furthermore, current evidence indicates that RUNX2 is a critical pathological factor in human metastatic breast, pancreatic, thyroid, prostate and colon cancer cells [34–37]. Thus, it

is likely that RUNX2 is closely involved in malignant cancer cell proliferation, chemoresistance, migration and invasion. To overcome the malignant phenotypes of human cancers, a precise understanding of the molecular mechanism(s) with respect to how aggressive cancers develop and maintain resistance to chemotherapeutic agents is required. As noted above, chemoresistance of cancerous cells is often attributed to an impaired functioning of p53 as a result of genetic mutation and/or sequestration by the other proteins. Recently, we described that RUNX2 attenuates p53-dependent apoptotic cell death in response to DNA damage [38], indicating that RUNX2 contributes to chemoresistance by inhibiting p53.

In the present study, we report that RUNX2 has the ability to suppress transcriptional activity as well as ADR-mediated induction of TAp73, thereby inhibiting the proper DNA damage response of cancerous cells.

Results

Simultaneous induction of TAp73 and RUNX2 during ADR-mediated cell death

To determine whether a functional interaction exists between pro-apoptotic TAp73 and pro-oncogenic RUNX2 during the DNA damage response, we investigated the expression level of TAp73 and RUNX2 in response to ADR. Accordingly, human osteosarcoma-derived *p53*-proficient U2OS cells were exposed to increasing doses of ADR. Consistent with our recent observations [38], U2OS cells underwent cell death after ADR treatment (Fig. 1). Under our experimental conditions, non-apoptotic cell death was barely detectable, as examined by annexin V and propidium iodide (PI) double-staining experiments. Whole cell lysates and total RNA were then prepared and analyzed by immunoblotting and RT-PCR, respectively. As shown in Fig. 2A, ADR-mediated accumulation of γH2AX and cleaved poly(ADP-ribose) polymerase (PARP) was detectable, indicating that DNA damage-induced cell death takes place in response to ADR. As expected, ADR treatment led to an induction of TAp73, as well as RUNX2, in association with a remarkable upregulation of p53/TAp73-target gene products, such as $p21^{WAF1}$ and BAX. Additionally, RT-PCR analysis revealed that ADR-dependent induction of TAp73 and RUNX2 is regulated at the transcription level (Fig. 2B).

Because p53 was also induced and phosphorylated at Ser-15 in response to ADR, it is likely that U2OS cells undergo cell death in a p53 and/or a TAp73-dependent manner. To confirm whether TAp73 could play a central role in the regulation of ADR-mediated cell death, U2OS cells were transfected with control small interfering RNA (siRNA) or with siRNA targeting *p73*. Transfected cells were then treated with or without ADR. Twenty-four hours after treatment, whole cell lysates and total RNA were extracted and analyzed for the expression of p53/TAp73-target genes. As seen in Fig. 3A, knockdown of *p73* suppressed an ADR-mediated induction of $p21^{WAF1}$ and BAX, whereas ADR-dependent upregulation of RUNX2 was basically unaffected. RT-PCR analysis demonstrated that depletion of *p73* impairs ADR-dependent transcriptional upregulation of various p53/TAp73-target genes, including $p21^{WAF1}$, *14-3-3σ*, *BAX*, *PUMA* and *NOXA*, indicating that, similar to p53, TAp73 is

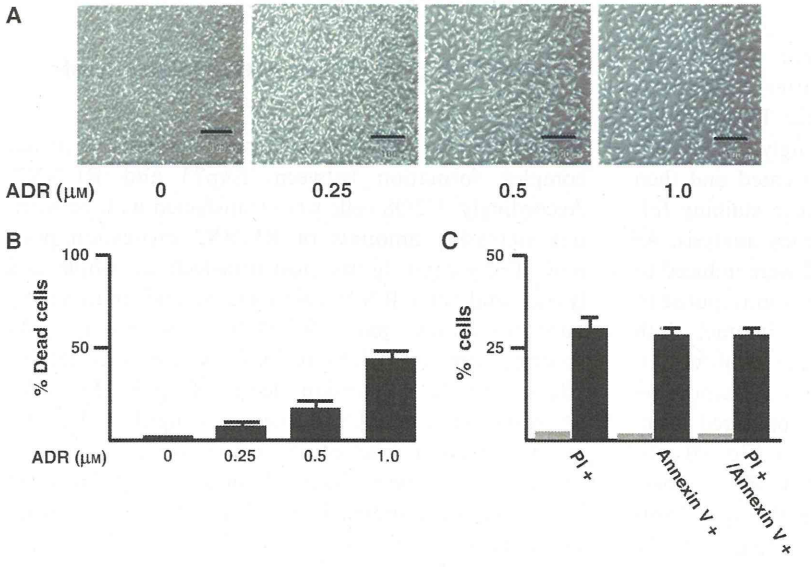

Fig. 1. U2OS cells undergo cell death in response to ADR. (A) Phase-contrast micrograph. U2OS cells were treated with the indicated concentrations of ADR or left untreated. Twenty-four hours after treatment, phase-contrast micrographs were taken. Scale bar = 100 μm. (B) Trypan-blue exclusion assay. U2OS cells were treated as described in (A). Twenty-four hours after treatment, cells were trypsinized and stained with 0.4% of trypan blue. Cells restricting trypan-blue entry were considered viable. (C) Annexin V and PI double staining. U2OS cells were treated with 0.5 μM of ADR (filled boxes) or left untreated (gray boxes). Twenty-four hours after treatment, cells were subjected to annexin V and PI double staining.

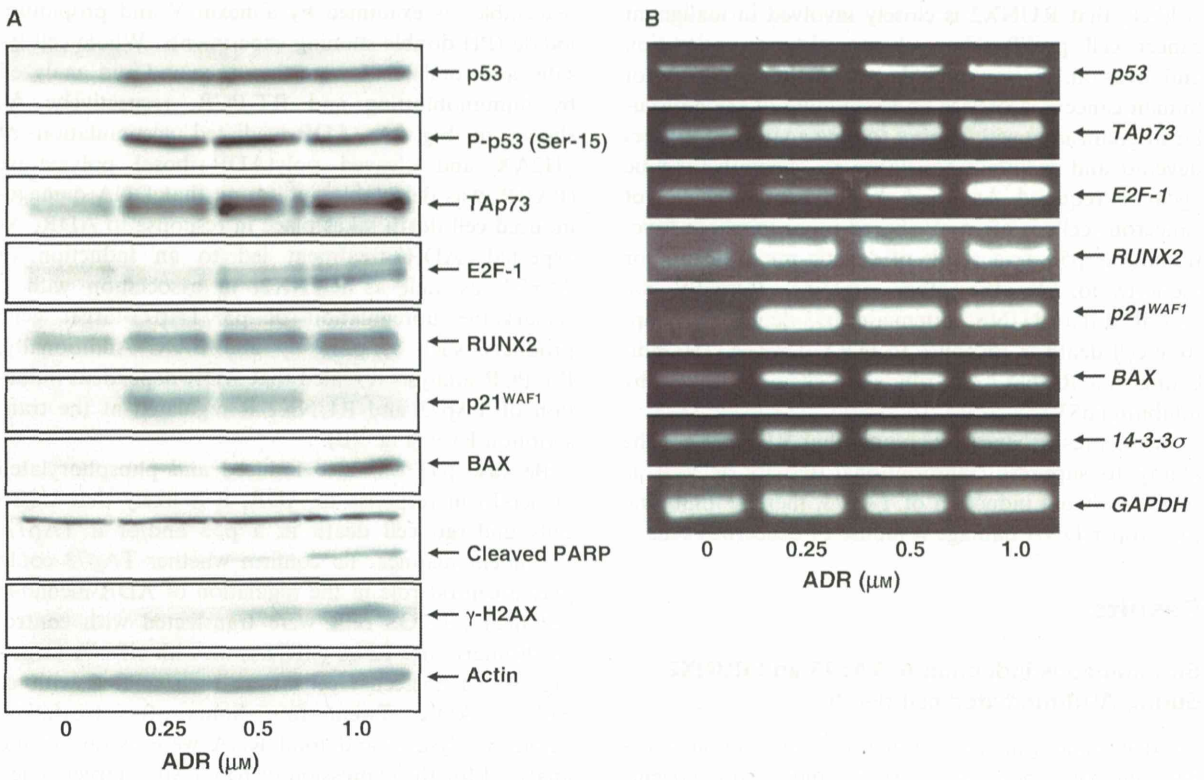

Fig. 2. ADR-mediated induction of TAp73 and RUNX2 in U2OS cells. U2OS cells were exposed to the indicated concentrations of ADR. Twenty-four hours after treatment, whole cell lysates and total RNA were prepared and subjected to (A) immunoblotting and (B) RT-PCR, respectively. Actin and *GAPDH* were used as a loading and an internal control, respectively.

required for ADR-mediated DNA damage response (Fig. 3B).

Complex formation between TAp73 and RUNX2 in response to ADR

The above observations showing that TAp73 and RUNX2 are simultaneously induced after ADR treatment prompted us to examine whether TAp73 could form a complex with RUNX2. Accordingly, U2OS cells were stimulated with ADR or left untreated and then subjected to indirect immunofluorescence staining followed by subsequent confocal microscopy analysis. As shown in Fig. 4A, TAp73 and RUNX2 were induced to accumulate and co-localize in cell nucleus in response to ADR, suggesting that TAp73 might interact with RUNX2 in the cell nucleus. To further confirm this possibility, we performed co-immunoprecipitation experiments using whole cell lysates prepared from ADR-treated U2OS cells. As shown in Fig. 4B, the anti-p73 immunoprecipitates contained the endogenous RUNX2. Similaly, the reciprocal experiments demonstrated that TAp73 is co-precipitated with the endogenous RUNX2. Intriguingly, we failed to detect RUNX2/TAp73 complex in the absence of ADR (data not shown). Thus, our present results imply that TAp73 forms a complex with RUNX2 in cell nucleus in response to DNA damage.

RUNX2 inhibits the transcriptional activity of TAp73

We next investigated a functional consequence of the complex formation between TAp73 and RUNX2. Accordingly, U2OS cells were transfected with or without increasing amounts of RUNX2 expression plasmid. Forty-eight hours post-transfection, whole cell lysates and total RNA were isolated and analyzed by immunoblotting and RT-PCR, respectively. As described previously [38], RUNX2 had an undetectable effect on the expression level of p53 (Fig. 5A). Overexpression of RUNX2 caused a marked decrease in the expression level of p53/TAp73-target genes, and similar results were also obtained in *p53*-deficient human lung carcinoma H1299 cells (data not shown). Of note, overexpression of RUNX2 in U2OS cells

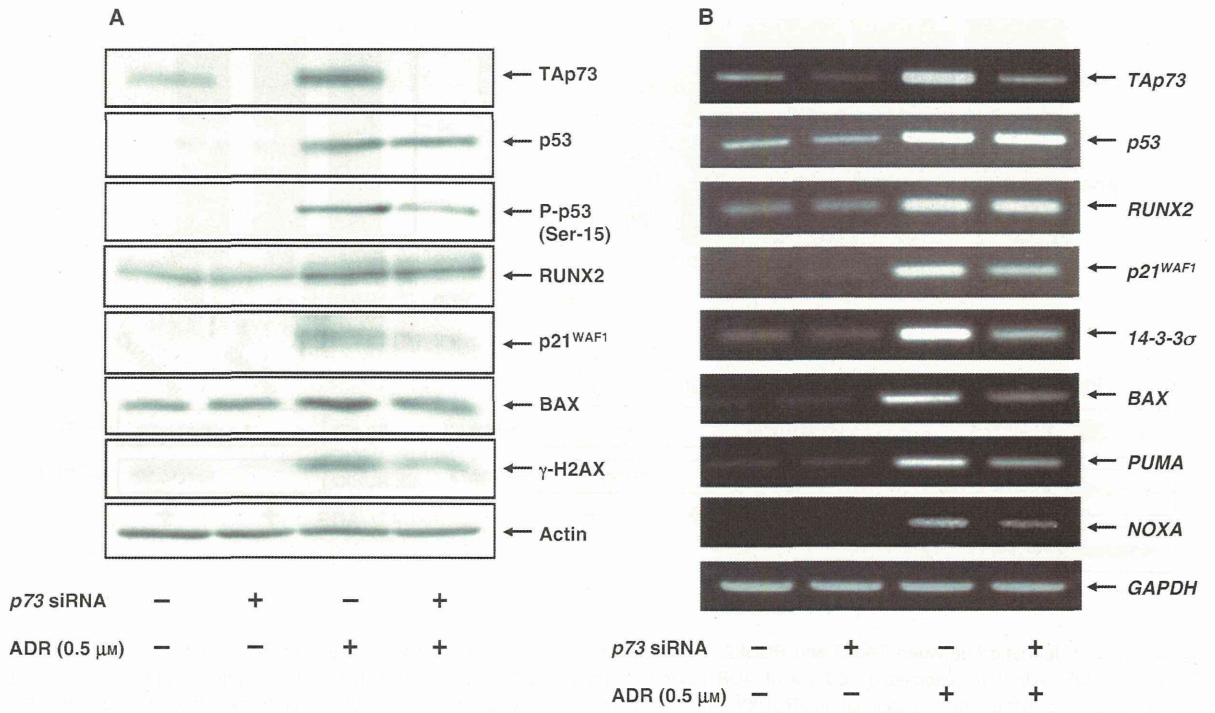

Fig. 3. Knockdown of *p73* attenuates ADR-mediated induction of p53/TAp73-target gene expression. U2OS cells were transfected with control siRNA or with siRNA against *p73*. Twenty-four hours after transfection, cells were treated with 0.5 μM of ADR or left untreated. Twenty-four hours after treatment, whole cell lysates and total RNA were extracted and processed for (A) immunoblotting and (B) RT-PCR, respectively.

resulted in an accelerated cell proliferation in a dose- and time-dependent fashion (Fig. 5B,C), raising the possibility that RUNX2-mediated downregulation of p53/TAp73-target gene products might contribute to the promotion of cell proliferation. Because U2OS and H1299 cells expressed wild-type TAp73, it is likely that, in addition to p53, RUNX2 might also inhibit the transcriptional activity of TAp73, thereby enhancing their unregulated cell proliferation.

To adequately address this issue, H1299 cells were transfected with the indicated combinations of the expression plasmids. Forty-eight hours post-transfection, whole cell lysates and total RNA were prepared and processed for immunoblotting and RT-PCR, respectively. As clearly shown in Fig. 6, overexpression of TAp73α stimulated the expression of p53/TAp73-target genes, such as *BAX*, *PUMA* and *NOXA*, whereas co-expression of TAp73α with RUNX2 markedly reduced their TAp73α-dependent transcriptional activation. Consistent with these results, luciferase reporter assays demonstrated that RUNX2 remarkably decreases TAp73α-mediated enhancement of luciferase activities driven by p53/TAp73-responsible human *BAX* and *NOXA* promoters in a dose-dependent manner (data not shown). These observations strongly suggest that RUNX2 inhibits the transcriptional activity of TAp73.

Knockdown of RUNX2 enhances ADR-mediated cell death in association with the transcriptional induction of TAp73

Recently, we reported that depletion of *RUNX2* in U2OS cells augments p53-dependent cell death after ADR exposure [38]. These observations led us to examine a possible effect of *RUNX2* knockdown on *TAp73* expression. Accordingly, U2OS cells were transfected with control siRNA or with siRNA targeting *RUNX2*, followed by incubation with or without ADR for 24 h. In accordance with our recent observations [38], RUNX2 was successfully knocked down under our experimental conditions (Fig. 7A) and RUNX2-depleted cells underwent cell death in response to ADR (42%) much more efficiently than ADR-treated control cells (24%), as examined by DNA ladder formation (Fig. 7B) and terminal deoxynucleotidyl transferase dUTP nick end labeling (TUNEL) staining (Fig. 8). To check whether silencing of

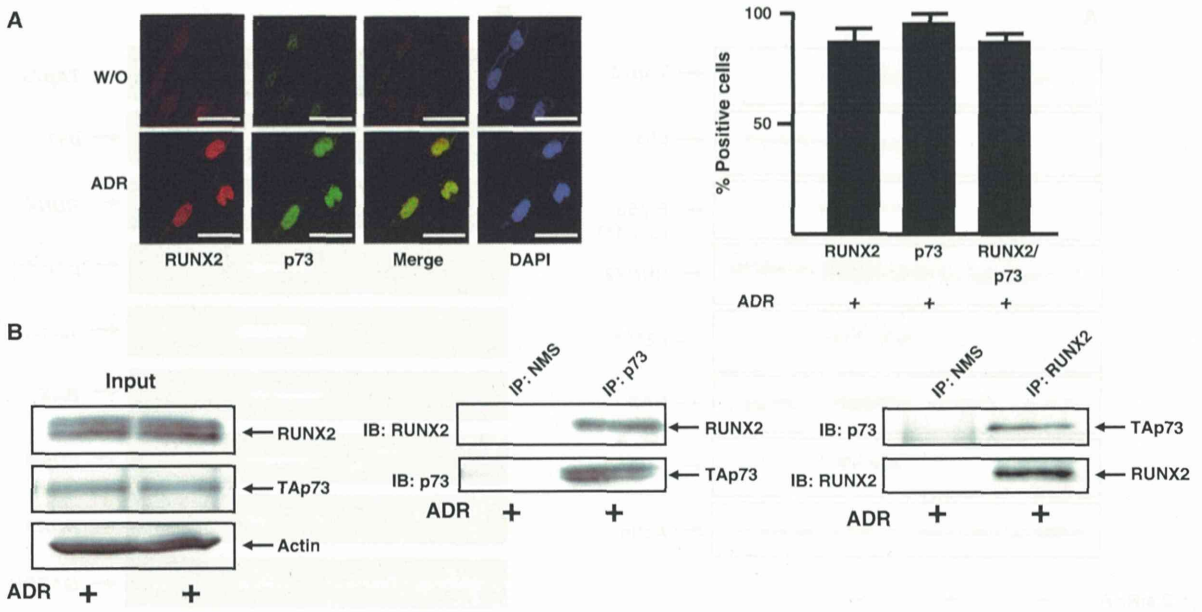

Fig. 4. Complex formation between TAp73 and RUNX2 in response to ADR. (A) Nuclear co-localization of TAp73 with RUNX2 after ADR exposure. U2OS cells were exposed to 0.5 μM of ADR (lower) or left untreated (upper). Twenty-four hours after treatment, cells were simultaneously incubated with monoclonal anti-RUNX2 (red) and polyclonal anti-p73 (green) antibodies. Cell nuclei were stained with DAPI (blue). Merged images (yellow) indicated the nuclear co-localization of TAp73 with RUNX2. Scale bar = 25 μm (magnification, × 630) (left). Percentages of RUNX2-, p73- or RUNX2/p73-positive cells were indicated (right). (B) Co-immunoprecipitation. An equal amount of whole cell lysates prepared from ADR-treated U2OS cells was immunoprecipitated with normal mouse serum (NMS) or with monoclonal anti-p73 antibody. The immunoprecipitates were analyzed by immunoblotting with the indicated antibodies (middle). The reciprocal experiments (right) and 1 : 20 inputs (left) are also shown.

RUNX2 could affect the expression level of *TAp73* after ADR treatment, total RNA was prepared and analyzed by RT-PCR. As clearly shown in Fig. 7C, ADR-mediated induction of p53/TAp73-target genes, such as $p21^{WAF1}$, *BAX* and *PUMA*, was further enhanced in *RUNX2*-knockdown cells. Of note, knockdown of *RUNX2* had a negligible effect on *p53* in cells exposed to ADR, whereas ADR-mediated upregulation of *TAp73* was further enhanced upon the silencing of RUNX2 expression. Additionally, depletion of *RUNX2* resulted in a slight increase in the steady-state expression level of *TAp73*. These observations suggest that RUNX2 has an ability to suppress ADR-dependent induction of *TAp73*, and TAp73 contributes at least in part to the higher sensitivity to ADR of *RUNX2*-depleted cells.

RUNX2 attenuates ADR-mediated cell death in association with the downregulation of TAp73

To further confirm whether RUNX2 could downregulate the expression of TAp73 during ADR-mediated cell death, U2OS cells were transfected with the empty plasmid or with RUNX2 expression plasmid. Twenty-four hours post-transfection, cells were incubated with or without 0.5 μM of ADR. As expected, overexpression of RUNX2 suppressed ADR-mediated cell death (Fig. 9), whereas ADR-mediated cell death was further stimulated in the presence of exogenous p53. Similar results were also obtained in a trypan-blue exclusion assay (data not shown). Under these experimental conditions, whole cell lysates and total RNA were prepared and analyzed for the expression level of TAp73 by immunoblotting and RT-PCR, respectively. As shown in Fig. 10A, ADR-mediated proteolytic cleavage of PARP, caspase-9 and induction of p53/TAp73-target gene products were notably suppressed by exogenous RUNX2. Similar results were also obtained in RT-PCR analysis (Fig. 10B). Intriguingly, ADR treatment led to a remarkable induction of TAp73, whereas ADR-mediated upregulation of TAp73 was impaired in cells expressing exogenous RUNX2. As expected, overexpression of RUNX2 also abrogated ADR-dependent transcriptional induction of *TAp73* and various p53/TAp73-target genes in H1299 cells (Fig. 11).

Taken together, our present findings strongly suggest that RUNX2 helps the resistance of cancerous cells to DNA damage by downregulation of TAp73.

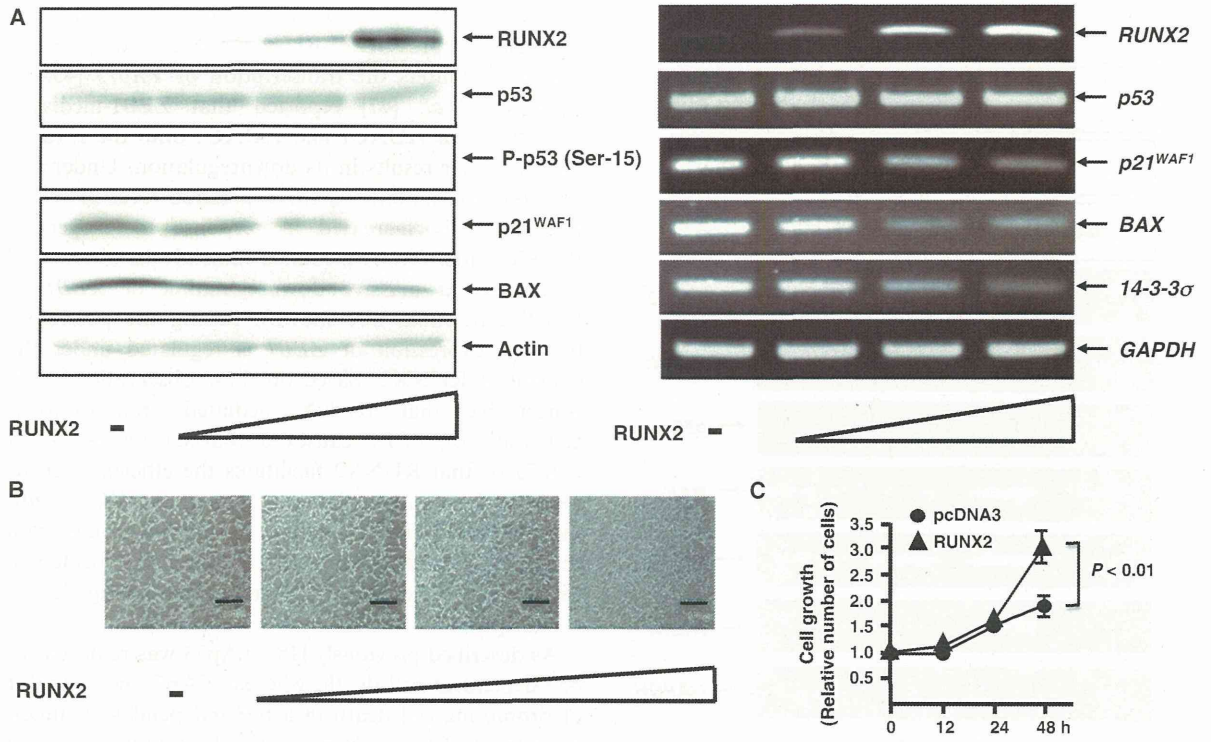

Fig. 5. RUNX2 represses the expression of p53/p73-target genes. (A) U2OS cells were transfected with or without the increasing amounts of the expression plasmid for RUNX2 (0.5, 1.0 or 2.0 μg). Forty-eight hours after transfection, whole cell lysates and total RNA were isolated and analyzed by immunoblotting (left) and RT-PCR (right), respectively. (B, C) RUNX2 promotes cell proliferation. U2OS cells were transfected as described in (A). Forty-eight hours after transfection, phase-contrast micrographs were taken. Scale bar = 100 μm (B). U2OS cells were transfected with 2.0 μg of the expression plasmid encoding RUNX2. At the indicated time points, the number of viable cells was measured (C).

Discussion

In the present study, we report that the transcriptional activity and ADR-mediated induction of pro-apoptotic TAp73 are significantly impaired by RUNX2. Because RUNX2 prohibits both wild-type p53 and TAp73, it is likely that the inhibition of RUNX2 might be a promising anti-cancer therapy for chemoresistant malignant cancers.

It is well established that, similar to p53, TAp73 is activated through DNA damage-mediated post-translational modifications such as phosphorylation and acetylation. For example, TAp73 was tyrosine phosphorylated at Tyr-99 by nonreceptor tyrosine kinase c-Abl in response to DNA damage, and c-Abl-mediated phosphorylation of TAp73 enhanced its stability as well as its transcriptional activity [39–41]. Alternatively, Costanzo *et al.* [42] demonstrated that DNA damage-induced acetylation of TAp73 at Lys-321, Lys-327 and Lys-331 stimulates its pro-apoptotic activity. According to our immunoprecipitation experiments, we successfully detected RUNX2/TAp73 complex in cells exposed to ADR (Fig. 4). By contrast, we failed to detect RUNX2/TAp73 complex in untreated cells, which might the result of the low expression level of RUNX2 and TAp73 or the absence of post-translationally modified active TAp73. Because RUNX2 significantly reduced the transcriptional activity of TAp73, it is likely that RUNX2 could preferentially associate with the transcriptionally active form of TAp73. Although plausible, this possiblity remains to be tested experimentally.

According to the results of the present study, overexpression of RUNX2 suppressed the ADR-dependent induction of *TAp73* and siRNA-mediated knockdown of *RUNX2* further enhanced ADR-dependent upregulation of *TAp73*, indicating that RUNX2 might repress *TAp73* expression at the transcritional level. In support of this notion, luciferase reporter assays demonstrated that luciferase activity driven by human *TAp73*

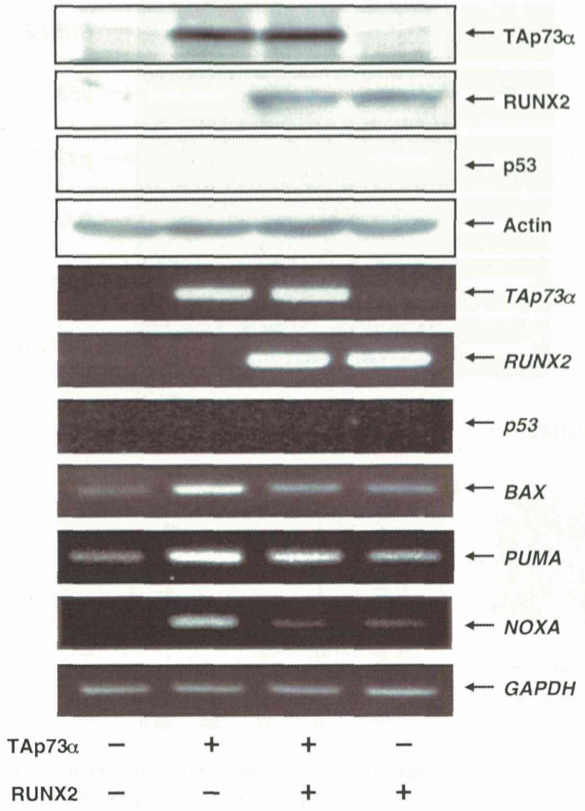

Fig. 6. RUNX2 inhibits the transcriptional activity of TAp73. H1299 cells were transfected with the indicated combinations of the expression plasmids. Forty-eight hours after transfection, whole cell lysates and total RNA were prepared and subjected to immunoblotting (upper) and RT-PCR (lower), respectively.

promoter (-2713/+20) is remarkably reduced in response to increasing amounts of exogenous RUNX2 (data not shown). Intriguingly, we identified several putative RUNX2-recognition sites (ACC(A/G)CA) within this promoter region (data not shown). RUNX/CBFβ complex is known to activate or repress the transcription of key regulators of growth, survival and differentiation pathways [43]. Recently, McGee-Lawrence *et al.* [44] reported that RUNX2 represses the transcription of its target genes by recruiting histone deacetylases (HDACs) to their promoters. We have also found that RUNX2 interacts with HDAC6, thereby inhibiting the transcription of p53/TAp73-target genes in response to DNA damage [38]. It is possible that RUNX2 downregulates the transcription of *TAp73* by recruiting HDACs to the putative RUNX2-binding site located within *TAp73* promoter region; however, additional experiments are required to adequately address this issue.

Alternatively, it has been demonstrated that transcriptional repressor ZEB1 which has anti-apoptotic potential, inhibits the transcription of *TAp73* [45,46]. Aghdassi *et al.* [47] reported that ZEB1-mediated recruitment of HDAC1 and HDAC2 onto the *E-cadherin* promoter results in its downregulation. Under our experimental conditions, the expression level of *ZEB1* was markedly increased in response to exogenous RUNX2, and siRNA-mediated knockdown of *RUNX2* resulted in a massive downregulation of *ZEB1* in U2OS cells (data not shown), raising the possibility that the expression of *ZEB1* is regulated under the control of RUNX2. Based on these observations, it is conceivable that RUNX2-mediated transcriptional activation of *ZEB1* causes a marked repression of *TAp73* or that RUNX2 facilitates the efficient recruitment of the repressor complex containing ZEB1 onto the putative RUNX2-binding site within 5′-upstream region of *TAp73* and/or ZEB1-binding site located in the first intron of *TAp73*, thereby attenuating *TAp73* transcription.

As described previously [18], TAp73 was required for p53-dependent cell death, whereas TAp73 was capable of promoting cell death in a p53-independent manner. In support of these observations, the overexpression of TAp73 alone in *p53*-deficient pancreatic cancer cells triggered cell death [48]. In addition, Willis *et al.* [49] demonstrated that TAp73 exerts its growth-suppressive activity in cancerous cells expressing mutant p53. Previously, Chen *et al.* [50] found that p53 transactivates *TAp73* through a functional p53-responsible element located within its 5′-upstream region. Under our experimental conditions, overexpression of FLAG-p53 stimulated transcription of *TAp73* in U2OS cells (data not shown). Given that TAp73 acts as an essential cofactor for p53 [18], RUNX2 knockdown-mediated enhancement of pro-apoptotic activity of p53 might be at least in part attiributed to p53-dependent induction of TAp73. It was worth noting that siRNA-mediated knockdown of *p73* strongly suppresses ADR-dependent upregulation of p53/TAp73-target gene expression even in the presence of active p53 (Fig. 3), implying that TAp73 plays a critical role during ADR-mediated cell death. Because *TAp73* is rarely mutated in a variety of human cancers [16], it is likely that silencing of *RUNX2* enhances chemosensitivity of malignant cancers expressing functionally impaired-p53 through up-regulation of TAp73.

In summary, we provided evidence showing that RUNX2 downregulates TAp73 in response to DNA damage. Therefore, we propose that silencing of *RUNX2* might be a novel strategy for improving chemosensitivity of malignant cancers.

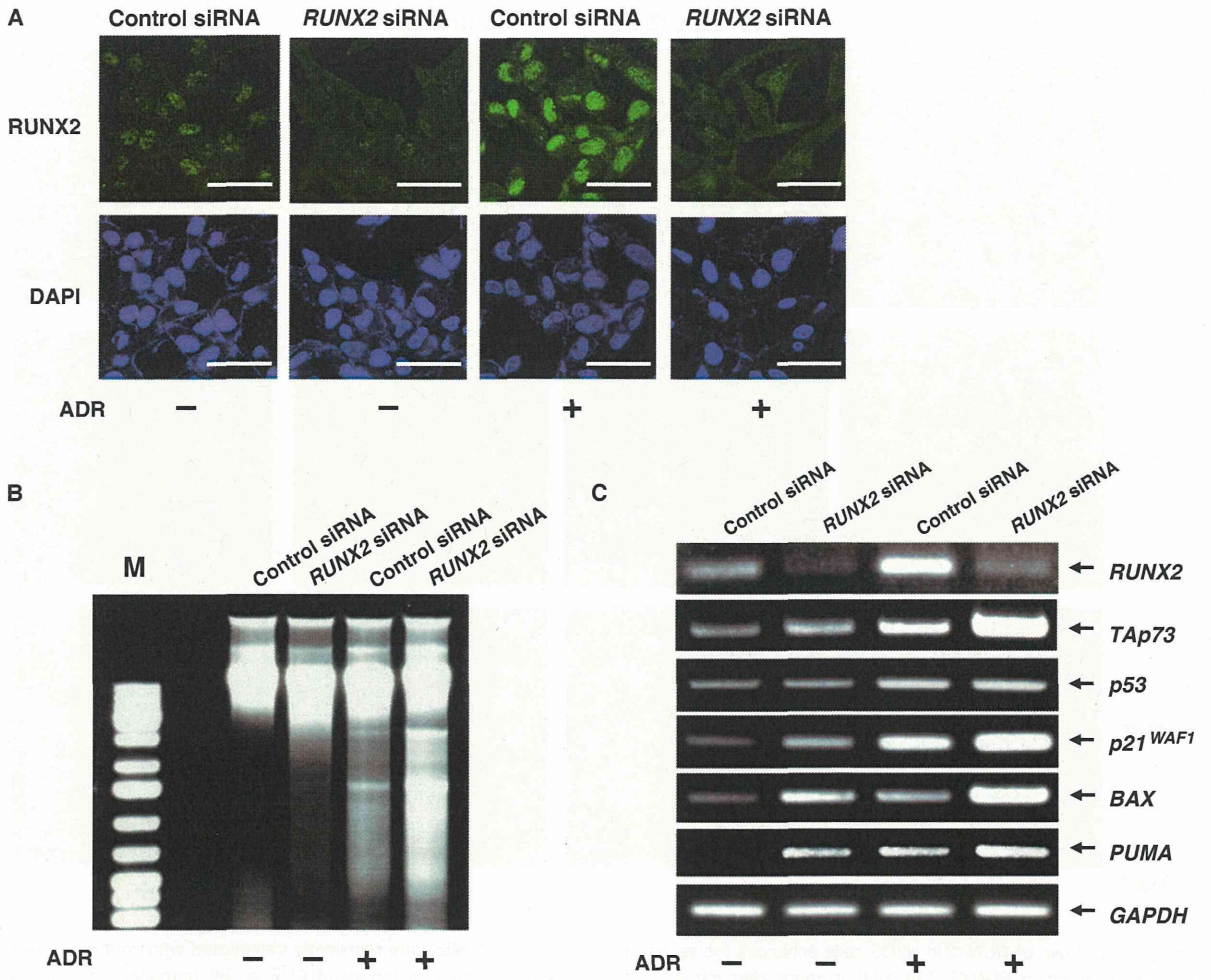

Fig. 7. siRNA-mediated knockdown of *RUNX2* enhances ADR-dependent cell death and expression of *TAp73*. (A) Knockdown of *RUNX2*. U2OS cells were transfected with control siRNA or with siRNA against *RUNX2*. Twenty-four hours after transfection, cells were treated with 0.5 μM of ADR or left untreated. After 24 h of incubation, cells were stained with anti-RUNX2 antibody (green). Cell nuclei were stained with DAPI (blue). Scale bar = 25 μm. (B) Genomic DNA fragmentation. U2OS cells were transfected as described in (A). Twenty-four hours post-transfection, cells were exposed to 0.5 μM of ADR or left untreated. Twenty-four hours after treatment, attached and floating cells were collected, and their genomic DNA was prepared and analyzed by 1% agarose gel electrophoresis. (C) RT-PCR analysis of the endogenous *TAp73*. U2OS cells were transfected as described in (A). Transfected cells were treated with 0.5 μM of ADR or left untreated. Twenty-four hours after treatment, total RNA was prepared and subjected to RT-PCR analysis.

Experimental procedures

Cells and transient transfection

p53-proficient human osteosarcoma-derived U2OS and *p53*-deficient human lung carcinoma-derived H1299 cells were grown in Dulbecco's modified Eagle's medium supplemented with heat-inactivated 10% FBS (Invitrogen, Carlsbad, CA, USA) and penicillin-streptomycin at 37 °C in 5% CO_2. For transient transfection, cells were transiently transfected with the indicated combinations of the expression plasmids by using Lipofectamine 2000 reagent in accordance with the manufacturer's instructions (Invitrogen). The expression plasmids used in the present study were: pcDNA3 empty plasmid, pcDNA3-TAp73α and pcDNA3-RUNX2.

Trypan-blue exclusion assay

The number of dead cells was determined by the trypan-blue exclusion assay. Cells were exposed to the indicated concentrations of ADR. Twenty-four hours after the treatment, cells were trypsinized and stained with trypan-blue (0.4%) at room temperature for 10 min. Cells restricting trypan-blue entry were considered viable.

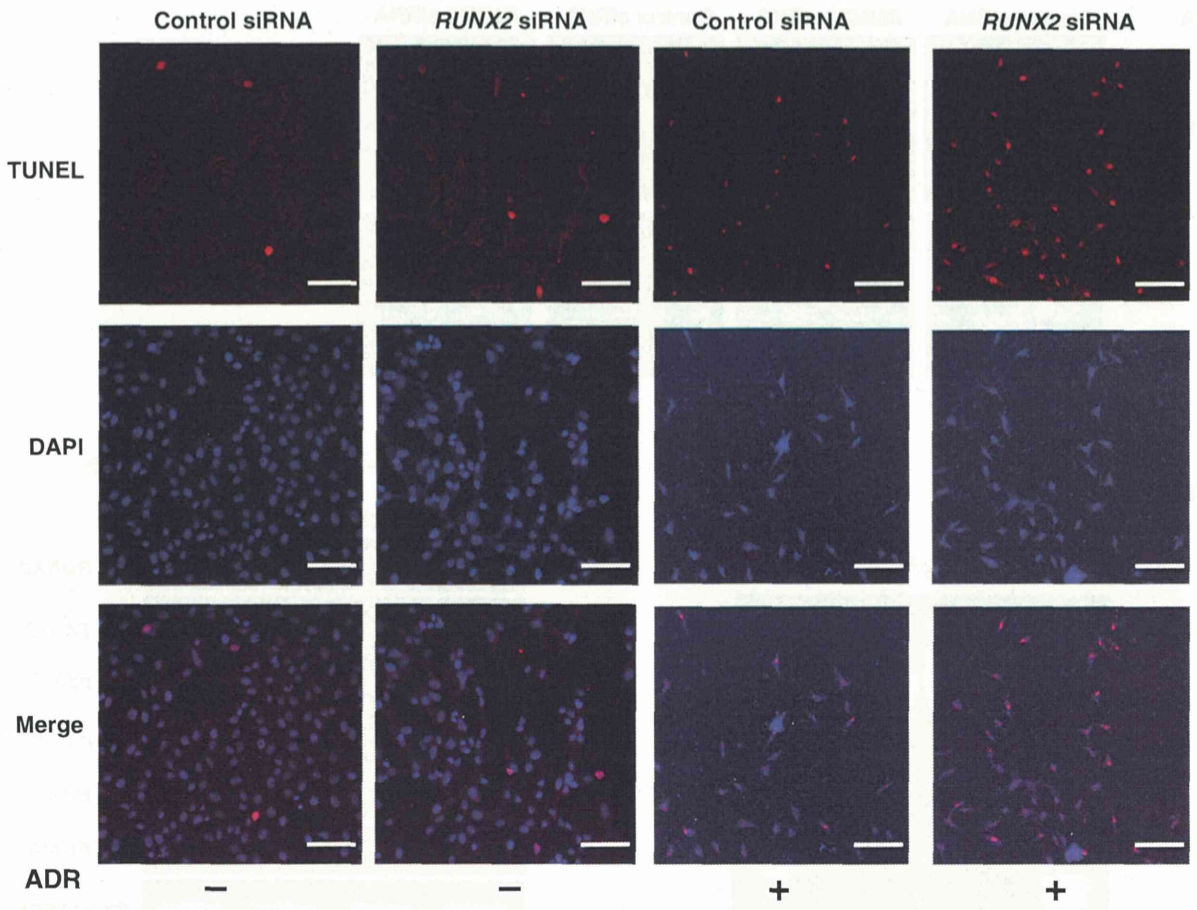

Fig. 8. Knockdown of *RUNX2* in U2OS cells enhances the sensitivity to ADR. U2OS cells were transiently transfected with control siRNA or with siRNA targeting *RUNX2*. Twenty-four hours after transfection, cells were treated with 0.5 μM of ADR or left untreated. Twenty-four hours after treatment, cells were subjected to TUNEL assay, and number of TUNEL-positive cells (red) was scored. Cell nuclei were stained with DAPI. Scale bar = 50 μm (magnification, × 100).

Annexin V and PI double staining

U2OS cells were treated with the indicated concentration of ADR or left untreated. Twenty-four hours after treatment, cells were washed in PBS and incubated with annexin V-FITC solution containing PI (50 $\mu g \cdot mL^{-1}$) at room temperature for 5 min in accordance with the manufacturer's instructions (PromoKine, Heiderberg, Germany). After the incubation, cells were washed in PBS, fixed in 2% formaldehyde at room temperature for 30 min and then observed under a confocal microscope (Leica, Milton Keynes, UK).

RNA extraction and RT-PCR

Total RNA was prepared from the indicated cells using RNeasy mini kit (Qiagen, Hilden, Germany) in accordance with the manufacturer's instructions. The integrity of total RNA was verified by visualization of rRNAs after electrophoresis in agarose gel. One microgram of total RNA for each sample was reverse-transcribed using SuperScript II reverse transcriptase (Invitrogen) in the presence of random primers. The resultant cDNA was subjected to PCR-based amplification using the specific primer sets for *TAp73*, 5′-TCTGGAACCAGACAGCACCT-3′ (sense) and 5′-GTG CTGGACTGCTGGAAAGT-3′ (antisense); *p53*, 5′-CTGC CCTCAACAAGATGTTTTG-3′ (sense) and 5′-CTATCTG AGCAGCGCTCATGG-3′ (antisense); *RUNX2*, 5′-TCTG GCCTTCCACTCTCAGT-3′ (sense) and 5′-GACTGGCG GGGTGTAAGTAA-3′ (antisense); *p21WAF1*, 5′-ATGAA ATTCACCCCCTTTCC-3′ (sense) and 5′-CCCTAGGCTG TGCTCACTTC-3′ (antisense); *14-3-3σ*, 5′-GAGCGAAAC CTGCTCTCAGT (sense) and 5′-CTCCTTGATGAGGTG GCTG-3′ (antisense); *BAX*, 5′-TTTGCTTCAGGGTTTCA TCC-3′ (sense) and 5′-CAGTTGAAGTTGCCGTCAGA-3′ (antisense); *PUMA*, 5′-GCCCAGACTGTGAATCCTGT-3′ (sense) and 5′-TCCTCCCTCTTCCGAGATTT-3′ (antisense);

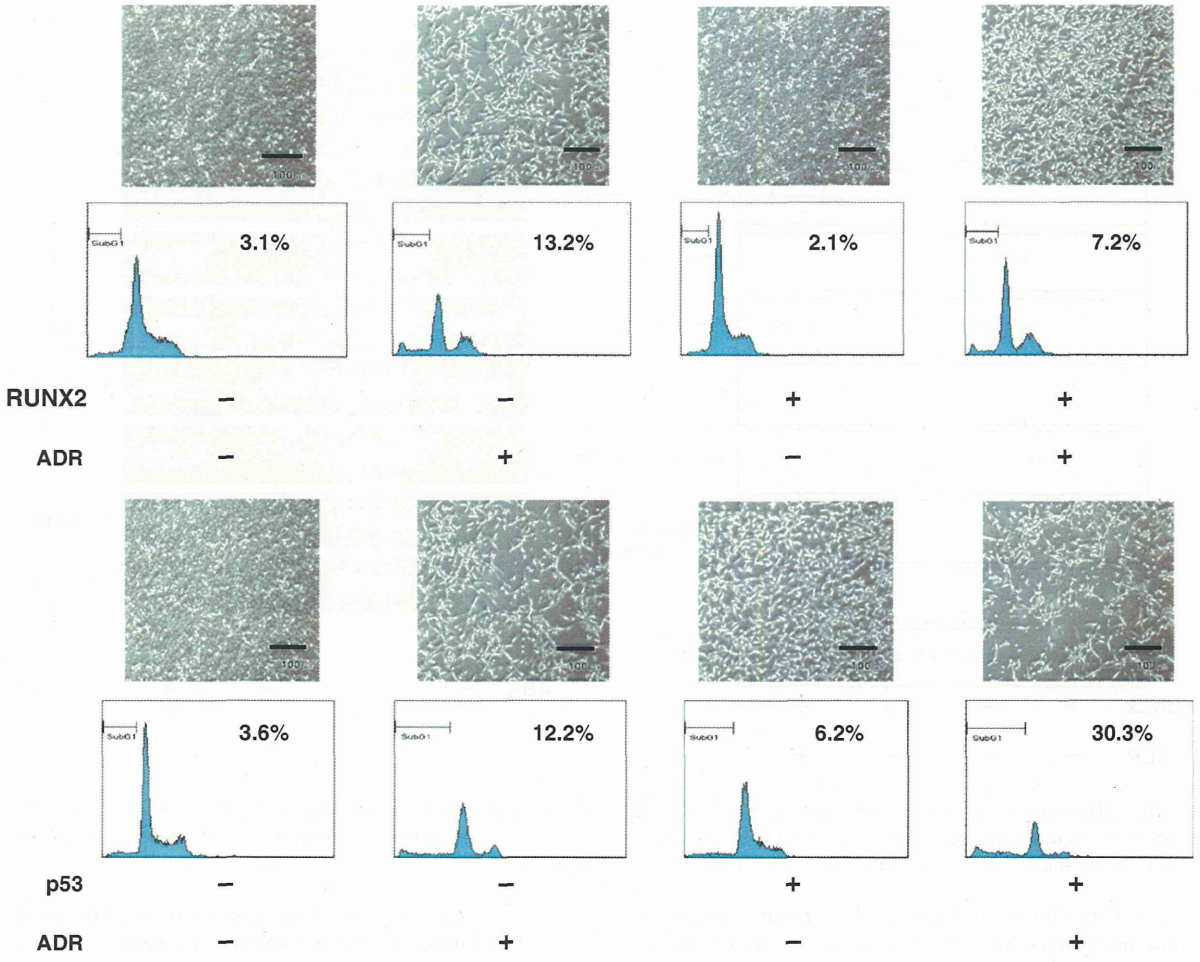

Fig. 9. RUNX2 prohibits ADR-mediated cell death. U2OS cells were transfected with the empty plasmid, the expression plasmid for RUNX2 (upper panels) or with the expression plasmid for p53 (lower panels), followed by additional incubation with or without 0.5 μM of ADR. Twenty-four hours after treatment, attached and floating cells were collected and analyzed by fluorescence-activated cell sorting.

NOXA, 5′-CTGGAAGTCGAGTGTGCTACT-3′ (sense) and 5′-TCAGGTTCCTGAGCAGAAGAG-3′ (antisense); *GAPDH*, 5′-ACCTGACCTGCCGTCTAGAA-3′ (sense) and 5′-TCCACCACCCTGTTGCTGTA-3′ (antisense). The PCR products were electrophoresed on 1.5% agarose gels and their amounts were evaluated by staining with ethidium bromide. *GAPDH* was used as an internal control.

Immunofluorescence

Cells were exposed to 0.5 μM of ADR or left untreated. Twenty-four hours after treatment, cells were washed twice in ice-cold PBS, fixed in 3.7% folmaldehyde in PBS at room temperature for 30 min, permeabilized with 0.1% Triton X-100 in PBS at room temperature for 5 min and then blocked with 3% BSA in PBS at room temperature for 1 h. After blocking, cells were washed in ice-cold PBS and simultaneously incubated with mouse monoclonal anti-RUNX2 (8G5; Medical & Biological Laboratories, Nagoya, Japan) and rabbit polyclonal anti-p73 (Bethyl Laboratories, Montgomery, TX, USA) antibodies at room temperature for 1 h followed by the incubation with rhodamine-conjugated goat anti-mouse IgG and FITC-conjugated goat anti-rabbit IgG (Invitrogen) at room temperature for 1 h. After the extensive washing, cell nuclei were stained with 4′,6-diamidino-2-phenylindole (DAPI) (Vector Laboratories, Peterborough, UK). Fluorescent images were captured using a confocal microscope.

Immunoblot analysis

Cells were washed twice in ice-cold PBS and immediately lysed in Laemmli buffer as described previously [38]. Equal amounts of cell lysates were resolved by 10% SDS/PAGE and electro-transferred onto poly(vinylidene difluoride) membrane. Immunoblot analyses were performed as